

# A hierarchical Bayesian model for predicting ecological interactions using evolutionary relationships

Mohamad Elmasri<sup>1,\*</sup>, Maxwell Farrell<sup>2</sup>, and David A. Stephens<sup>1</sup>

<sup>1</sup>Department of Mathematics and Statistics,

<sup>2</sup>Department of Biology

<sup>1,2</sup>McGill University,

805 Sherbrooke Street West, Montreal, QC H3A 0B9, CA

July 8, 2022

## Abstract

Identifying undocumented or potential future interactions among species is a challenge facing modern ecologists. Recent link prediction methods rely on trait data, however large species interaction databases are typically sparse and covariables are limited to only a fraction of species. On the other hand, evolutionary relationships among species, encoded as phylogenetic trees, can act as proxies for underlying traits and historical patterns of parasite sharing among hosts. We show that using a network-based conditional model, phylogenetic information provides significant predictive power in a recently published global database of host-parasite interactions. Drawing from evolutionary biology, we find that applying alternative evolutionary models to the phylogeny greatly improves it. To further improve on the phylogeny-only model, we use a hierarchical Bayesian latent score framework for bipartite graphs that accounts for the number of interactions per species, as well as the host dependence informed by phylogeny. Combining the two information sources yields significant improvement in predictive accuracy over each of the submodels alone. As many interaction networks are constructed from presence-only data, we extend the model by integrating a correction mechanism for missing interactions, which proves valuable in reducing uncertainty in unobserved interactions.

**Keywords**— network graph, Bayesian hierarchical model, ecological interactions, link prediction, host-parasite network

---

\*Corresponding author mohamad.elmasri@mail.mcgill.ca

# 1 Introduction

Currently, most ecological networks are only partially observed and fully characterizing all interactions via systematic sampling involves substantial effort and investment that is not feasible in most situations (Jordano, 2015). Approaches to predict highly probable, yet previously undocumented links in interaction networks are an integral component of proactive surveillance systems for emerging diseases (Farrell et al., 2013). As we enter into a data revolution in the study of biodiversity (La Salle et al., 2016), global databases of species interactions are becoming readily available (Poelen et al., 2014; Stephens et al., 2017; Wardeh et al., 2015).

There are many potential approaches for link prediction in networks, but often these are based on features or traits of the interacting nodes Dallas et al. (2017); Olival et al. (2017); Ricci et al. (2011). For large-scale ecological datasets, traits determining species interactions are often unknown or are available only for a limited subset of species (Morales-Castilla et al., 2015). When trait information is limited, evolutionary relationships among species may be used as a proxy. Phylogenetic trees are a representation of the evolutionary relationships among species, which provide means to quantify ecological similarity (Wiens et al., 2010). Just as many species traits co-vary with phylogeny, species interactions are also phylogenetically structured in both antagonistic (ex. herbivory, parasitism) and mutualistic (ex. pollination, seed dispersal) networks (Gómez et al., 2010). Incorporating phylogeny into ecological link prediction has the added benefit that it is universally applicable across diverse species.

In this paper we demonstrate a phylogeny-based framework for predicting undocumented links using a recent global database of host-parasite interactions (Stephens et al., 2017). In host-parasite networks, parasite community similarity is often well predicted by evolutionary distance among hosts (Davies and Pedersen, 2008; Gilbert and Webb, 2007). We focus on wild mammal hosts that are most closely related to domesticated ungulates and carnivores, as these species are known to harbour diseases of concern for humans and livestock (Cleaveland et al., 2001), and include many species that are threatened with extinction due to infectious diseases (Pedersen et al., 2007). We incorporate phylogenetic information as a weighted network, where weights quantify pairwise host similarities. Such approach allows for easy expansion to different forms of dependency, if phylogenetic information is unavailable, or of other dependency structures are preferred. We show that phylogenetic information alone can generate accurate predictions using a naive point estimate. We can make predictions using an untransformed phylogeny, however, evolutionary biologists have developed methods of transforming phylogenies to represent alternative modes of evolution (Harmon et al., 2010; Pagel, 1999). Rescaling the tree using these approaches can alter the dependence structure among hosts, and may yield better predictions that can be interpreted in the context of a model of trait evolution. We

extend our naive approach by estimating a tree transformation parameter, which results in posterior distributions for the probabilities of each host-parasite interaction.

We then show this phylogeny-only model can be extended to use properties of the network structure to model species likelihood of interaction, mimicking that of network-based models such as [Bickel and Chen \(2009\)](#); [Chung and Lu \(2006\)](#); [Hoff \(2005\)](#); [Hoff et al. \(2002\)](#). To facilitate the construction of the full joint distribution, we first augment the model using a hierarchical latent variable framework. The latent variable acts as an underlying scoring system, with higher scores attributed to more probable links. Second, we apply the iterated conditional modes algorithm of [Besag \(1974\)](#) to deal with the conditional dependency imposed by phylogeny, and include a method to account for uncertainty in unobserved interactions. Our approach allows for robust predictions for large species interaction networks with limited covariate data, and can be extended to any bipartite network with a dependence structure for one of the interacting classes.

## 2 Data

We illustrate our framework on the recently published Global Mammal Parasite Database version 2.0 (GMPD), described in [Stephens et al. \(2017\)](#). The GMPD contains over 24,000 documented associations between hosts and their parasites collected from published reports and scientific studies. The assumed interactions are based on empirical observations of associations between host-parasite pairs using a variety of evidence types (visual identification, serological tests, or detection of genetic material from a parasite species in one or more host individuals). Associations are reported along with their publication reference. More than one reference might be reported per association, and by aggregation one can determine the count of unique references per interaction. The GMPD gathers data on wild mammals and their parasites (including both micro and macroparasites), which is separated into three primary databases based on host taxonomy: Primates, Carnivora, and ungulates (terrestrial hooved mammals in the orders Artiodactyla and Perissodactyla). We restricted our analyses to the ungulate and Carnivora subsets because of prior experience with these data [Farrell et al. \(2015\)](#), and tractability of the size of the resulting network.

The GMPD was used to construct a bipartite binary matrix, where rows represent hosts and columns parasites and documented associations are indicated by 1. We construct host pairwise similarities as the inverse of phylogenetic distances calculated from the mammal phylogeny of [Fritz et al. \(2009\)](#), which involved collapsing host subspecies to species. We excluded parasites that were not reported to species level. This resulted in a GMPD subset with 4775 pairs of interactions among 251 hosts and 1552 parasites. Out of these 1552 parasites, 809 were found to associate with a single host ( $\approx 52\%$ )

One of the models proposed in [Section 3.1](#) (the phylogeny-only model) can only be

specified for multi-host parasites. Thus, for the purpose of model comparison, we remove single-host parasites, reducing the GMPD to 3966 interactions among 246 hosts and 743 parasites. In subsequent analyses we refer to the database without single-host parasites, unless otherwise specified.

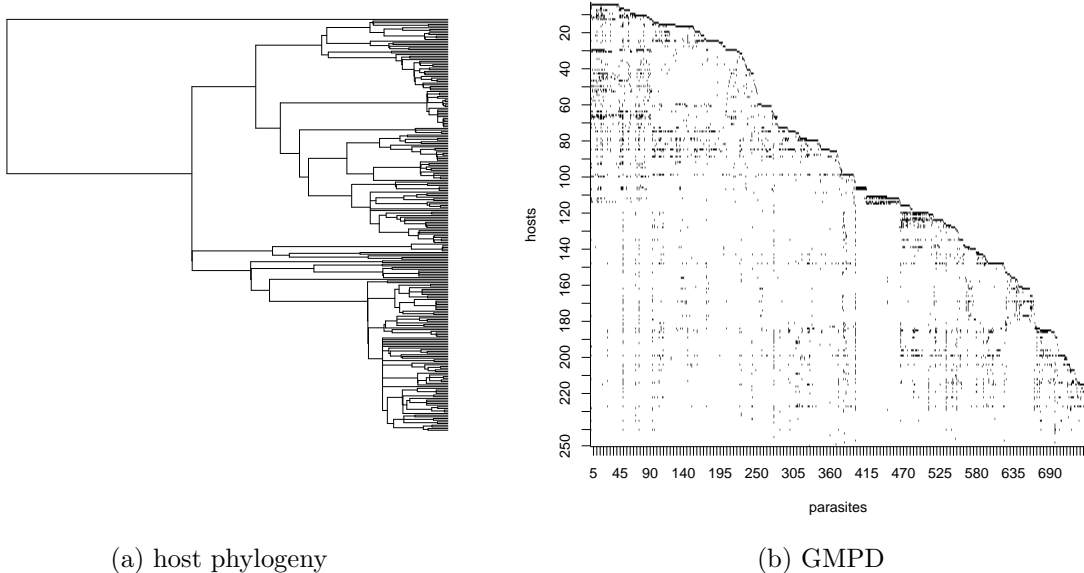


Figure 1: a) The host phylogeny and b) the left ordered interaction matrix  $\mathbf{Z}$  of the GMPD.

Figure 1 shows the left-ordered interaction matrix  $\mathbf{Z}$  of GMPD, and corresponding host phylogeny. The matrix  $\mathbf{Z}$  is sparse, and the degree distributions of both hosts and parasites exhibit a power-law structure (Appendix Figure 14).

### 3 Bayesian hierarchical model for prediction of ecological interactions

#### 3.1 Network-based latent score model

Conditional modelling is common in many biological network models, where the class of auto-models of Besag (1974) and latent space models of Hoff et al. (2002) are widely applied. One example is the use of a network-based auto-probit model in Jiang et al. (2011), where a protein-protein association network is used as a prior to predict protein functional roles conditional on the roles of neighbouring proteins. Such network-based models rely on a pre-existing binary or weighted network with a clearly defined neighbourhood structure. Probabilities are then derived by averaging over neighbouring nodes.

Evolutionary distances among species, represented by phylogeny, translate to a fully connected weighted network. Since pairwise distances among species are measured relative their most recent common ancestor, the same distance may be assigned to multiple host pairs. In this case a threshold method can be applied, but with two main drawbacks: i) the complexity of inferring the threshold parameter, and ii) the interpretation of the threshold with respect to evolutionary distance.

In the case of host-parasite interactions, parasites are often found to interact with closely related hosts, but in some cases may make large jumps in phylogeny and interact with distantly related hosts (Parrish et al., 2008). To account for such behaviour and to overcome the drawbacks of the threshold method, we let the probability of a host-parasite interaction be driven by the sum of evolutionary distances to the documented hosts of the parasite.

Let  $\mathbf{Z}$  be an  $H \times J$  host-parasite interaction matrix, where the binary variable  $z_{hj}$  denotes whether an interaction between host  $h$  and parasite  $j$  has been observed. Quantifying divergences starting from the root of the tree, let  $T_{hi}$  be the pairwise phylogenetic distances among hosts  $h$  and  $i$ , and their common ancestor  $k$  in millions of years, such that  $T_{hi} = T_{hk} + T_{ik} = (t_h - t_k) + (t_i - t_k)$ .

The most basic point estimate of the conditional probability of host  $h$  interacting with parasite  $j$  is defined as

$$\mathbf{P}(z_{hj} = 1 \mid \mathbf{z}_{(-h)j}) = 1 - \exp(-\delta_{hj}), \quad \delta_{hj} = \sum_{\substack{i=1 \\ i \neq h}}^H \frac{z_{hj}}{T_{hi}}, \quad (1)$$

where  $\mathbf{z}_{(-h)j}$  is the set of interactions of the  $j$ -th parasite among the  $H$  hosts ( $\mathbf{z}_{.j} = (z_{1j}, \dots, z_{Hj})$ ), excluding that of the  $h$ -th host.

The point estimate in (1) allocates higher probabilities when closely related hosts interact with a given parasite, or when many distantly related hosts also interact. The more distantly related the hosts are, the smaller the value of  $1/T_{hi}$ . The next section introduces an approach that allows us to transform and accounting for uncertainty in the phylogenetic distances  $T_{hi}$ .

### 3.1.1 Evolutionary models and phylogeny transformations

A focus of macroevolutionary research has been to develop models of trait evolution. A well known model and default in many ecological applications is Brownian motion, however, transformations of the phylogenetic tree can be made to reflect alternatives in the tempo of evolution. Transformations that can be formulated with only a single transformation parameter include the early-burst (EB), delta, kappa, lambda, and the Ornstein-Uhlenbeck transformations (Harmon et al., 2010; Pagel, 1999). Each model scales phylogenetic distances according to a model of evolution. Rather than treating

the distances of  $T_{hi}$  in (1) as fixed, a tree transformation can be used. We term this the phylogeny-only model and define it as

$$\mathbf{P}(z_{hj} = 1 \mid \mathbf{z}_{(-h)j}) = 1 - \exp(-\delta_{hj}), \quad \delta_{hj} = \sum_{\substack{i=1 \\ i \neq h}}^H \frac{z_{hj}}{\phi(T_{hi}, \eta)}, \quad (2)$$

where  $\phi(T_{hi}, \eta)$  is the transformed distance under a given evolutionary model controlled by a single parameter  $\eta$ .

In an effort to decide which transformation to use, we exclude the kappa transformation as it was designed to represent a speciation model of evolution with change occurring at speciation events, which makes the transformation highly sensitive to missing species in the phylogeny (Bapst, 2014). We then implement a simple grid search over the parameter space in (2) for the remaining models and find most known tree transformations provide no or negligible improvement in predictive power for our data over the original tree structure (Appendix Figure 9). However, the EB model stands-out by displaying a non-trivial convex relationship with predictive power.

The EB model allows evolutionary change to accelerate or decelerate through time, for example, evolutionary change may be fastest early in a clades history, but slows through time. The rate of change in the EB model is adjusted by a single parameter  $\eta \in \mathbb{R}$ , with positive values of  $\eta$  indicating that evolution is faster earlier in history, while negative values suggests the opposite. Figure 2 illustrates the EB transformation for different values of  $\eta$  in the Carnivora subset of the GMPD.

Under the EB model, the phylogenetic distance between a pair of hosts  $(h, i)$  with a most recent common ancestor  $k$ , is quantified as

$$\phi(T_{hi}, \eta) = \phi(T_{hk}, \eta) + \phi(T_{ik}, \eta) = \frac{1}{\eta}(e^{\eta t_h} - e^{\eta t_k}) + \frac{1}{\eta}(e^{\eta t_i} - e^{\eta t_k}). \quad (3)$$

Thus, for  $\eta = 0$ , EB reduces to original tree distance as  $\phi(T_{hi}, 0) = T_{hi}$ . While this represents one form of uncertainty in the phylogenetic distances, future work may also incorporate uncertainty in the posterior distribution of phylogenetic trees resulting from Bayesian phylogenetic inference. This could account for uncertainties in tree topology as well as distances.

### 3.1.2 Full model

Species interactions can be predicted using phylogenetic trees, though not completely, since interactions can also be driven by traits that are independent of phylogeny. In general, many network-based models assume that edge probabilities are driven by independent node affinity parameters, for example Bickel and Chen (2009); Chung and Lu (2006) and many others. Here we model the conditional probability of an interaction

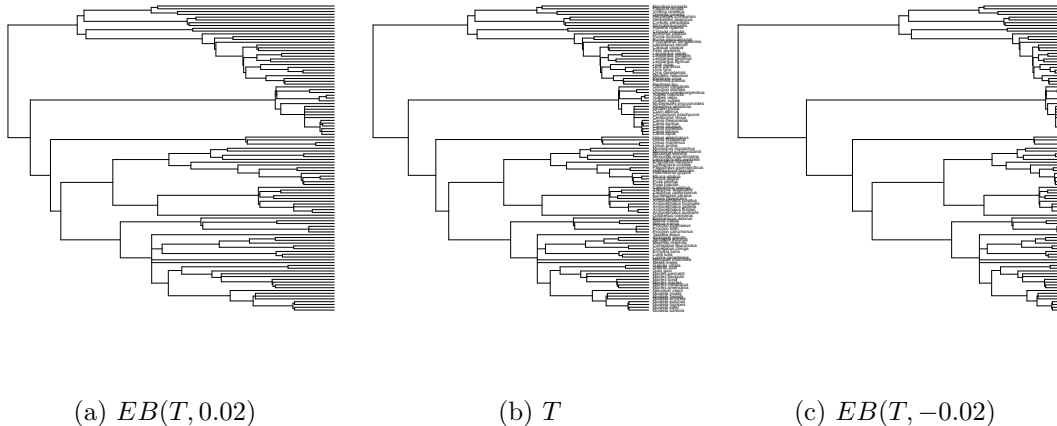


Figure 2: Examples of the early-burst transformation in the Carnivora subset of GMPD.

by combining both sources of information: phylogenetic distances and individual species affinities. Affinity parameters govern the general propensity for each organism to interact with members of the other class, with larger affinities correlated with larger probabilities and a higher likelihood that an organism will interact. Let  $\gamma_h > 0$  be the affinity parameter of host  $h$ , and  $\rho_j > 0$  of parasite  $j$ . The full conditional model is then

$$\mathbf{P}(z_{hj} = 1 \mid \mathbf{Z}_{-(hj)}) = 1 - \exp(-\gamma_h \rho_j \delta_{hj}(\eta)), \quad (4)$$

with  $\delta_{hj}(\eta)$  as in (2) under the EB transformation, here with a default value of  $\delta_{hj}(\eta) = 1$  if no neighbouring interactions exist.  $\mathbf{Z}_{-(hj)}$  is the interaction matrix  $\mathbf{Z}$  excluding  $z_{hj}$ .

The model of (4) can be reduced to an affinity-only model, setting  $\delta_{hj}(\eta) = 1$ , which can result in a workable network prediction model, as has been shown in the literature on exchangeable random networks, such as the work of Hoff et al. (2002). However, affinity-only models tend to generate adjacency matrices with many hyperactive columns and rows. This is due to the fact that whenever a node has a sufficiently high affinity parameter it forms edges with almost all other nodes, which is likely to be unrealistic for most global ecological networks, including host-parasite interactions. In Section 5.2 we show that both models, the affinity-only and phylogeny-only, independently result in suitable predictive models that represent some variation in the data. However, each model captures different characteristics of the graph and by layering them we obtain a non-trivial improvement.

Finally, we find it advantageous to use latent variables in modelling the binary variables  $z_{hj}$ . This facilitates the construction of the network joint distribution while accounting for Markov network dependence imposed by  $\delta_{hj}(\eta)$ . In addition, the latent variable construction becomes essential in addressing the ambiguity associated with the case when  $z_{hj} = 0$ , which entails two possibilities: a yet to be observed positive interaction, or a

true absence of interaction due to incompatibility (implemented in Section 4).

Thus, for each  $z_{hj}$  we define latent score  $s_{hj} \in \mathbb{R}$  such that

$$z_{hj} = \begin{cases} 1 & \text{if } s_{hj} > 0 \\ 0 & \text{otherwise,} \end{cases} \quad (5)$$

where  $s_{hj} \in \mathbb{R}$  is a continuous random variable acting as a latent score determining the probability of  $z_{hj}$  being an interaction. Although unobserved,  $s_{hj}$  completely determines the binary variables  $z_{hj}$ . Therefore, the conditional model in (4) can be completely specified in terms of the latent score as

$$\mathbf{P}(z_{hj} = 1 \mid \mathbf{Z}_{-(hj)}) = \mathbf{E}[\mathbb{I}_{\{s_{hj} > 0\}} \mid \mathbf{Z}_{-(hj)}] = \mathbf{P}(s_{hj} > 0 \mid \mathbf{S}_{-(hj)}) \quad (6)$$

where  $\mathbf{S}_{-(hj)}$  represents the interaction matrix  $\mathbf{S}$  excluding  $s_{hj}$ , replacing  $\mathbf{Z}$  as it carries the same probability events.

Given the construction above, we use a zero-inflated Gumbel distribution for the latent score with the following density

$$\mathbf{p}(s_{hj} \mid \mathbf{S}_{-(hj)}) = \tau_{hj} \exp(-s_{hj} - \tau_{hj} e^{-s_{hj}}) \mathbb{I}_{\{s_{hj} > 0\}} + \exp(-\tau_{hj}) \mathbb{I}_{\{s_{hj} = 0\}}, \quad (7)$$

where  $\tau_{hj} = \gamma_h \rho_j \delta_{hj}(\eta)$ . Hence, the conditional joint distribution becomes

$$\mathbf{P}(z_{hj} = 1, s_{hj} \mid \mathbf{Z}_{-(hj)}) = \mathbf{P}(z_{hj} = 1 \mid s_{hj}) \mathbf{p}(s_{hj} \mid \mathbf{S}_{-(hj)}) = \mathbf{p}(s_{hj} \mid \mathbf{S}_{-(hj)}) \mathbb{I}_{\{s_{hj} > 0\}} \quad (8)$$

The proposed latent score model, though intricate in formulation, is no more inferentially complex than the auto-logit model of [Besag \(1974\)](#). The reasons we use it are: i) a simple joint distribution for each row of  $\mathbf{Z}$  conditional on all others; ii) a simple posterior distributions for the affinity parameters; and iii) the ability to correct for uncertainty using the latent score formulation.

Alternatively, one can adopt other network-based conditional models, such as the multivariate Gaussian latent variable with a conditional mean structure of [Jiang et al. \(2011\)](#). Such models are of a similar complexity to the phylogeny-only model in (2), modelling each column of  $\mathbf{Z}$  independently. Adding affinity parameters to a model with a neighbourhood dependence will increase complexity, but this also applies to alternative network-based conditional models.

### 3.2 Prior and Posterior distribution of choice parameters

The choice of a zero-truncated Gumbel was made to facilitate the construction of the joint distribution, in a manner similar to the Swendsen-Wang algorithm ([Swendsen and Wang,](#)



1987) where a product of densities transform to a sum in the exponential scale, improving the tractability of posteriors. Alternatively, the truncated exponential distribution can be used, as shown in Appendix B.2, though it does not admit the direct interpretability as a latent score as with the Gumbel distribution.

By the Hammersley-Clifford theorem (Robert and Casella, 2013), it is straightforward to verify that the joint distribution exists, as briefly shown in Appendix (B). Even though the form is complicated, we do not need to access the joint density and instead may use a Gibbs sampler as in Geman and Geman (1984). An iterative algorithm can then be used to sample from conditionally independent components of the joint distribution, with the posterior sample obtained by averaging. One example of such an approach is the iterated conditional modes (ICM) algorithm of Besag (1974).

In the proposed model the joint distribution of rows are conditionally independent given the rest. Let  $\mathbf{Z}_{-(h.)}$  be  $\mathbf{Z}$  excluding the  $h$ -th row  $\mathbf{z}_{h.}$ . With similar notations for  $\mathbf{S}$ , the joint distribution of the  $h$ -th row is

$$\mathbf{P}(\mathbf{z}_{h.}, \mathbf{s}_{h.} \mid \mathbf{Z}_{-(h.)}) = \gamma_h^{n_h} \left[ \prod_{j=1}^J (\rho_j \delta_{hj}(\eta))^{z_{hj}} \right] \exp \left( - \sum_{j=1}^J s_{hj} + \gamma_h \rho_j \delta_{hj}(\eta) e^{-s_{hj}} \right) \quad (9)$$

where  $n_h = \sum_{j=1}^J z_{hj}$  such that the row-wise joint posterior distribution is

$$\mathbf{P}(\mathbf{s}_{h.}, \gamma_h, \boldsymbol{\rho}, \eta \mid \mathbf{Z}) \propto \mathbf{P}(\mathbf{z}_{h.} \mid \mathbf{s}_{h.}) \mathbf{P}(\mathbf{s}_{h.} \mid \mathbf{S}_{-(h.)}, \gamma_h, \boldsymbol{\rho}, \eta) \mathbf{P}(\gamma_h) \mathbf{P}(\boldsymbol{\rho}) \mathbf{P}(\eta), \quad (10)$$

where  $\mathbf{P}(\mathbf{z}_{h.} \mid \mathbf{s}_{h.}) = \prod_{j=1}^J \mathbf{P}(z_{hj} \mid s_{hj}) = 1$ , and  $\boldsymbol{\rho}$  is the parasite affinity parameter set.

Using the ICM in a sweeping manner for  $h = 1, \dots, H$  rows of  $\mathbf{Z}$ , one samples  $\gamma_h$  from its full posterior, and  $\boldsymbol{\rho}^{(h)} = (\rho_1^{(h)}, \dots, \rho_J^{(h)})$  and  $\eta^{(h)}$  from their  $h$ -th row conditional posteriors. Obtaining an MCMC sample of  $\boldsymbol{\rho}$  and  $\eta$  is done by averaging over the  $H$  samples from the row posteriors.

For prior specifications we choose a gamma distribution for both affinity parameters because of their conjugacy property. Thus, let  $\gamma_h \stackrel{\text{iid}}{\sim} \text{Gamma}(\alpha_\gamma, \tau_\gamma)$  and  $\rho_j \stackrel{\text{iid}}{\sim} \text{Gamma}(\alpha_\rho, \tau_\rho)$ . The full posterior distributions of  $\gamma_h$  and the  $h$ -row partial posterior of  $\rho_j^{(h)}$ , respectively, are

$$\begin{aligned} \rho_j^{(h)} \mid \mathbf{z}_{h.}, \mathbf{s}_{h.} &\sim \text{Gamma} \left( \alpha_\rho + z_{hj}, \tau_\rho + \gamma_h \delta_{hj}(\eta) e^{-s_{hj}} \right), \\ \gamma_h \mid \mathbf{z}_{h.}, \mathbf{s}_{h.} &\sim \text{Gamma} \left( \alpha_\gamma + n_h, \tau_\gamma + \sum_{j=1}^J \rho_j \delta_{hj}(\eta) e^{-s_{hj}} \right). \end{aligned} \quad (11)$$

In the case of the scaling parameter  $\eta$  we assume a constant prior for simplicity and computational stability, although this could be readily modified to any subjective prior.

The latent score is updated, given all other parameters as

$$s_{hj} \mid z_{hj}, \mathbf{S}_{-(hj)} \sim \begin{cases} \chi_0 & \text{if } z_{hj} = 0 \\ \text{tGumbel}\left(\log \gamma_h \rho_j + \log \delta_{hj}(\eta), 1, 0\right) & \text{if } z_{hj} = 1, \end{cases} \quad (12)$$

where  $\chi_0$  is an atomic measure at zero and  $\text{tGumbel}(\tau, 1, 0)$  is the zero-truncated Gumbel with density

$$\frac{\exp(-(s - \tau + e^{-(s-\tau)}))}{1 - \exp(-e^\tau)} \chi_{(0, \infty)}(s).$$

The adaptive Metropolis-Hastings algorithm (Haario et al., 2001) within Gibbs is used to update the model parameter. For additional details on the model and the MCMC method sampling algorithm refer to Appendix A.

So far, we have assumed that the information given in  $\mathbf{Z}$  is definite, that the observed links are presences and unobserved ones are absences. However, as discussed previously, we believe this will not be the case for many ecological networks. The next section introduces a method for dealing with such cases.

## 4 Uncertainty in unobserved interactions

In ecological networks it is unlikely that all potential links will be represented or observed. Some unobserved exist but are undocumented due to limited or biased sampling, while others may be true absences or “forbidden” links (Morales-Castilla et al., 2015). Evidence used to support an interaction will vary depending on the nature of the system, but it is often assumed that an interaction exists if at least one piece of evidence indicates so (Jordano, 2015).

This raises concern about the uncertainty of interactions in two ways. The first is due to uncertainty in documented interactions as false positive detection errors may occur, potentially as a result of species misidentification, sample contamination, or in our case unanticipated cross-reactions in serological tests. We believe it would be useful for the scientific community to identify weakly supported interactions that may require additional supporting evidence, however our primary motivation is identification of “novel” interactions, which is complicated by uncertainty in unobserved interactions.

The second concern arises when unobserved associations are by default assumed to be true absences. As discussed earlier, ecological networks are often under-sampled, and some fraction of unobserved interactions may occur but are currently undocumented, or represent potential interactions that are likely to occur given sufficient opportunity. Based on this assumption we build a measure of uncertainty in unobserved interactions by modifying our proposed model in (4). In (5), we have assumed that  $\mathbf{P}(z_{hj} = 1 \mid s_{hj} > 0) = 1$ , a deterministic quantity given  $s_{hj}$ . Thus we have only sampled positive scores for

the case when  $z_{hj} = 1$ , as shown in (12). As a result, the posterior predictive distribution is only considered for the case when a pair has no documented associations ( $z_{hj} = 0$ ), and it is deterministic with probability 1 otherwise, underlining the assumption that the data is complete and trusted. In presence-only data, the objective is to model the non-trivial object  $\mathbf{P}(z_{hj} = 1, \text{“a missing link”} \mid s_{hj} > 0)$ . To account for such uncertainty, we attempt to approximate the proportion of interactions that are missing links in the latent space by measuring the percentage of positive scores where the input is 0 ( $z_{hj} = 0$ ) as

$$\mathbf{p}(z_{hj} = 0 \mid s_{hj}, g) = \begin{cases} 1, & \text{if } s_{hj} = 0, \\ g, & \text{if } s_{hj} > 0, \end{cases} \quad (13)$$

where  $g$  is the probability that an interaction is unobserved when the latent score indicates an interaction should exist. If  $g$  is large and close to 1, it is likely that many of the unobserved interactions could or should exist. Introducing  $g$  to the model affects all parameter estimates and the notion of  $\mathbf{Z}$ . Therefore, the posterior predictive distribution is now considered for both cases. For the case of a documented association, the probability of an interaction is defined in (4), and for the case of no documentation the same probability is weighted by  $g$  as shown in detail in (14).

This kind of construction has been used earlier by Weir and Pettitt (2000) when modelling spatial distributions to account for uncertainty in regions with unobserved statistics, and later by Jiang et al. (2011) in modelling uncertainty in protein functions.

## 4.1 Markov Chain Monte Carlo algorithm

Introducing a measure of uncertainty in the model does not alter the MCMC sampling schemes introduced in Section 3.2. The variables  $\gamma, \rho$  and  $\eta$  are still only associated with  $\mathbf{S}$ , nonetheless, by introducing the measure of uncertainty, the conditional sampling of each individual  $s_{hj}$  is now

$$\mathbf{p}(s_{hj} \mid \mathbf{S}_{-(hj)}, \mathbf{Z}, g) = \begin{cases} \frac{1}{\psi(\bar{s}_{hj})} \tau_{hj} \exp\left(-(s_{hj} + \tau_{hj} e^{-s_{hj}})\right), & s_{hj} > 0, \quad z_{hj} = 1, \\ 0, & s_{hj} = 0, \quad z_{hj} = 1, \\ \frac{g}{\theta(g, \bar{s}_{hj})} \tau_{hj} \exp\left(-(s_{hj} + \tau_{hj} e^{-s_{hj}})\right), & s_{hj} > 0, \quad z_{hj} = 0, \\ \frac{1}{\theta(g, \bar{s}_{hj})} 1 - \psi(\bar{s}_{hj}), & s_{hj} = 0, \quad z_{hj} = 0, \end{cases} \quad (14)$$

where  $\tau_{hj} = \gamma_h \rho_j \delta_{hj}^\eta$ ,  $\psi(\bar{s}_{hj}) = \int_0^\infty \mathbf{p}(s \mid \mathbf{S}_{-(hj)}) \mathbf{d}s = 1 - \exp(-\gamma_h \rho_j \delta_{hj}^\eta)$ , and  $\theta(g, \bar{s}_{hj}) = g\psi(\bar{s}_{hj}) + 1 - \psi(\bar{s}_{hj})$ .

Sampling the uncertainty parameter is performed using the row-wise conditional dis-

tribution as

$$\mathbf{P}(g \mid \mathbf{s}_{h.}, \mathbf{z}_{h.}) \propto \mathbf{P}(\mathbf{z}_{h.} \mid \mathbf{s}_{h.}, g) \mathbf{P}(\mathbf{s}_{h.} \mid \mathbf{S}_{-(h.)}) \cdot \mathbf{P}(g) \propto g^{N_{-+}} (1 - g)^{N_{++}}, \quad (15)$$

where  $N_{-+} = \#\{(h, j) : \mathbf{z}_{hj} = 0, s_{hj} > 0\}$ ,  $N_{++} = \#\{(h, j) : \mathbf{z}_{hj} = 1, s_{hj} > 0\}$ , and  $P(g)$  is a uniform. Since the sampling is done by iteratively cycling through the rows of  $\mathbf{Z}$ , as in the proposed ICM method, a sample of  $g$  is the average of the  $H$  row samples.

## 5 Results

### 5.1 Parameter estimation for the latent score full model

Using the GMPD we first fit the model proposed in Section 3.1. We run 10000 MCMC iterations and the same for burn-in for posterior estimates. In total we have  $J + H + 1$  parameters to estimate: an affinity parameter for each host and each parasite, and a tree scaling parameter for the host phylogeny.

Standard convergence diagnostics showed that all parameters had converged. It is worth noting that for the GMPD, the posterior distributions of the host parameters ( $\gamma$ ) show large variation, which reflects that some hosts are more likely to interact with parasites, or have been more intensively studied. The magnitude of the scaling parameter  $\eta$  is found to concentrate around 0.00815, indicating slightly accelerating evolution compared to the original tree. For additional convergence and diagnostic plots refer to Appendix D.

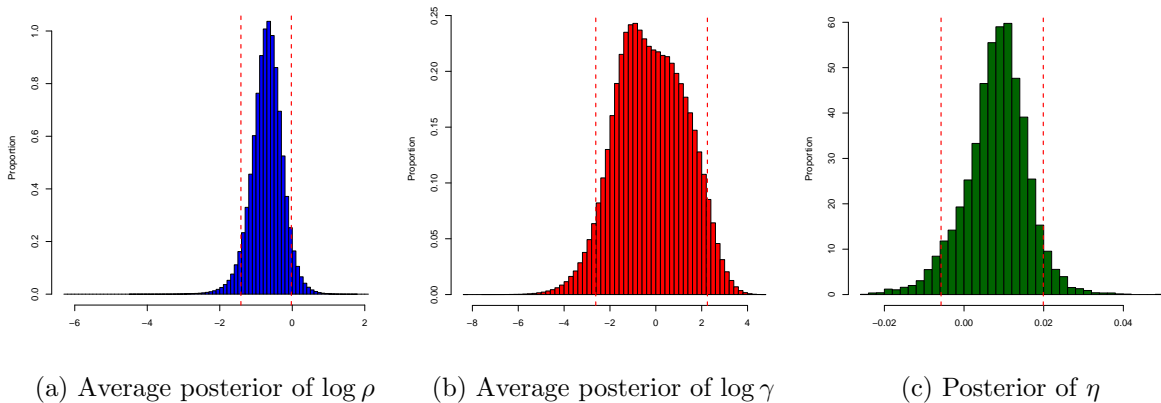


Figure 3: Posterior distributions for GMPD parameters.

### 5.2 Alternative models and comparison by cross-validation

To validate the predictive performance of the proposed latent score full model, we compare it to the two submodels of Section 3.1 (the affinity-only and the phylogeny-only models),

and to a nearest-neighbour (NN) algorithm. Finally, we compare the latent score full model to a NN algorithm, in which we set the distances between hosts proportional to the number of parasite species they share, also known as the Jaccard distance. This particular similarity matrix does not require additional data other than  $\mathbf{Z}$ . This similarity matrix determines the host dependence structure and thus, conditional on all the rest, we let the probability of a host-parasite interaction be equal to the average number of host-neighbours with documented association to the parasite, within the  $k$ -closest host-neighbours. These three variations are implemented using the presence-only matrix  $\mathbf{Z}$ .

The predictive performance of each model is evaluated using the average of 5-fold cross-validations, where each fold sets a proportion of the observed interactions ( $z_{hj} = 1$ ) in  $\mathbf{Z}$  to unknowns ( $z_{hj} = 0$ ) while attempting to predict them using the remaining interactions. We run a standard MCMC simulation to infer the parameters of interest under each fold, then the mean posterior probability of an interaction for each of the unknowns is calculated. By uniformly thresholding those probabilities from 0 to 1, where probabilities above the threshold are assumed to represent an interaction, we calculate the true positive and negative rates, and the false positive and negative rates. By this process, we finally obtain the receiver-operating characteristic (ROC) curves, and the posterior interaction matrix using the threshold that maximizes the area under the ROC curve (AUC).

The phylogeny-only model in (2) is ill-formulated for the case of single-host parasites, since  $\delta_{hj}(\eta) = 0$ . Therefore, for comparison across the models, each held-out portion is constructed to insure that at least two interactions are kept in each column of  $\mathbf{Z}$ . By this restriction, each fold held-out approximately 13% of documented associations. For single-host parasites,  $\delta_{hj}(\eta)$  is 0 as no other interaction information exists. In such cases we reduce the full model to the affinity-only model by setting  $\delta_{hj}(\eta)$  to 1.

Evident from 5-fold average ROC curves in Figure 4, the predictive performance of the latent score full model outperforms the NN algorithm and its two submodels. The NN algorithm performs almost equally to the affinity-only and phylogeny-only submodels. Nevertheless, neither of the two submodels performed on par with the full model, which confirms the notion that each of the simpler models captures different characteristics of the data, and layering them yields better results.

For a visual interpretation, Figure 5 illustrates posterior predictive matrices for the affinity-only (5a), phylogeny-only (5b) and the full model (8b). To show the full effect of different models, posterior probabilities for all interactions in  $\mathbf{Z}$ , observed and unobserved, are used to generate the the matrices in Figure 5. From these figures, the affinity-only model did not appear to account for any neighbouring structure and results in hyperactive hosts, while the phylogeny-only model based on host-neighbourhoods results in greater differences among parasites. The overall shape of the original  $\mathbf{Z}$  in Figure 1 is best captured by the full model.

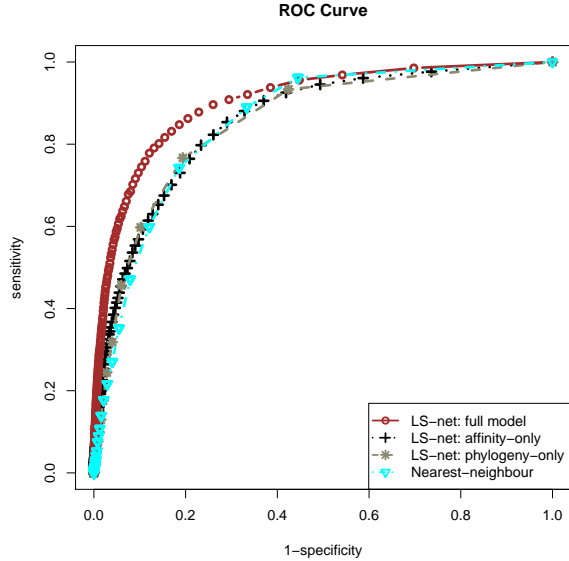


Figure 4: ROC comparison of the latent score network (LS-net) model with its two submodels and the an NN algorithm. The proposed LS-net full model in red, the affinity-only submodel in black, phylogeny-only variation in grey. The NN algorithm in cyan. All ROC curves are based on an average of 5-fold cross-validations.

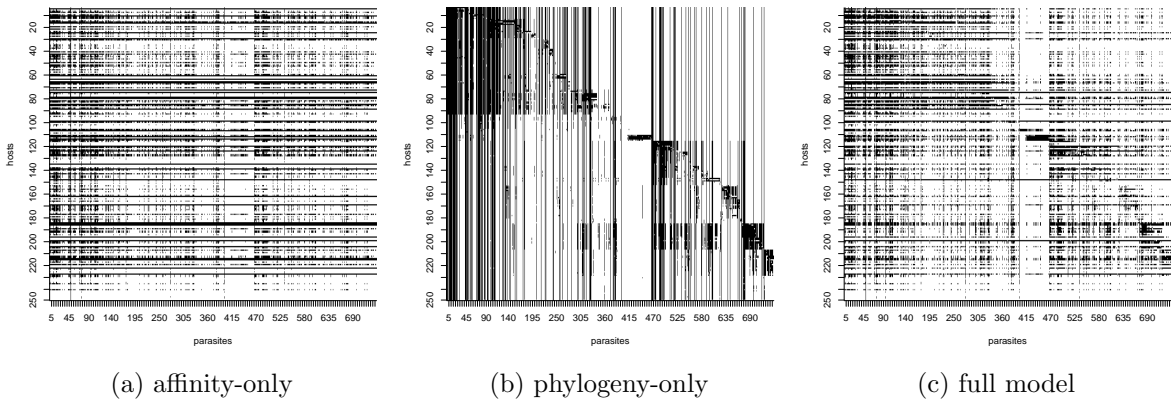


Figure 5: Posterior associations matrix comparison for the GMPD: between the affinity-only (left), phylogeny-only (middle) and full model (right).

For an analytical comparison, we followed the recommendation of [Demšar \(2006\)](#) to use the two-sided Wilcoxon signed rank test on the 5-fold cross-validations. We obtain a  $p$ -value of 0.043 when comparing the full model with the NN algorithm. Indicating, for a 5% level of significance, that the full model marginally outperforms the NN algorithm. When comparing the full model to the two submodels, the  $p$ -value is  $< 0.05$  across the board, suggesting a significant improvement obtained with the full model.

Single-host parasites comprise a non-negligible portion of the total pairwise interactions ( $\approx 17\%$ ), and including them in the calculation of host affinity parameters increases predictive performance, even though they are not considered part of the cross-validation

Table 1: Area under the curve and prediction values for tested models

Model	GMPD			
	no single-host parasites		with single-host parasites	
	AUC	% 1's recovered	AUC	% 1's recovered
full model	0.905	85.32	0.942	89.52
affinity-only	0.858	83.11	0.899	85.44
phylogeny-only	0.857	85.40	0.898	86.21
Nearest-neighbour	0.857	86.82	0.871	86.94

set.

To assess the effect of including single-host parasites on model performance, we repeated all analyses while keeping these in the original data. Table 1 shows the 5-fold average AUC and true positive prediction results when the single-host parasites are kept or removed from the GMPD. The predictive strength of the full model is now more evident. The increase in AUC for the full model is directly attributed to the inclusion of single-host parasites, since both the AUC and the percent of 1's recovered increased for the same held-out portion. For the other models, the AUC increase is coupled with a weaker improvement in the recovery of positive interactions. Since the single-host parasites are not part of the hold-out set, this improved AUC is due to the increased proportion of zeros in the larger database, as the held-out portion is kept constant.

### 5.3 Uncertainty in unobserved interactions

We improve our latent score model by accounting for uncertainty in unobserved interactions, as shown in Section 4. This addition increases the posterior predictive accuracy by estimating the proportion of missing interactions in the latent space, and reducing scores for unobserved interactions. Using the model in Section 4, we infer the uncertainty parameter  $g$  in the GMPD, using 5000 MCMC iterations with half as burn-in. The posterior mean of  $g$  is found to be 0.084 (posterior histograms in Figure 6). Documented associations in the GMPD are identified through systematic searches of peer-reviewed articles that support an interaction, therefore, we expect those associations to be of high confidence, reflecting the low value of  $g$ .

To show the improved predictive accuracy of this model, we divided GMPD into two sets, a training and a validation set. Since associations in the GMPD are sourced only from peer-reviewed articles, we were able to use information on article publication dates to create the training and test datasets. This mimics the discovery of interactions in the system rather than random hold-out of observations. Taking the earliest annotated year for each association we set the training set as all associations documented prior to and including 2004, and the validation set as all associations up to 2010. There are 4144 pairs of documented associations in the GMPD, including single-host parasites, up to

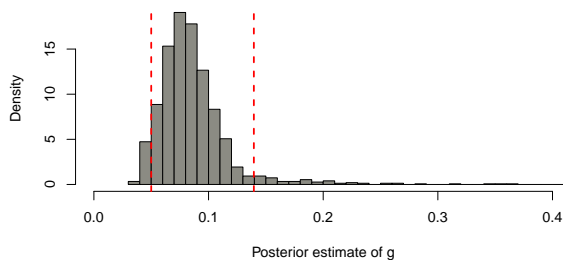
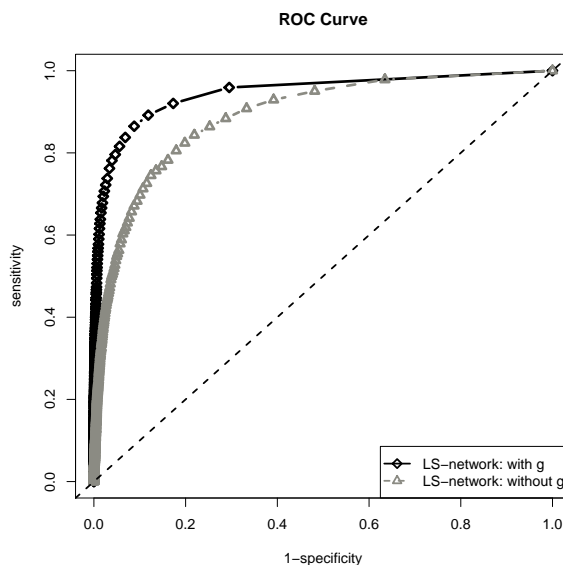


Figure 6: Posterior histogram for  $g$  for the GMPD.

and including 2004. By 2010, the associations increased to 4775, with 251 hosts and 1552 parasites, approximately a 15% increase. For the training sets using the GMPD up to 2004, we used an average of 5-fold cross-validations to estimate the parameters of the model, where each fold ran for 5000 iterations with half as burn-in. Since the full model is used, cross-validation is no longer restricted to multi-host parasites as in Section 5.2, nonetheless, to avoid empty columns at least one interaction is kept for each parasite.



(a) GMPD

Figure 7: Comparison of ROC curves for the full model with  $g$  (black) and without  $g$  (grey), for the 2010 GMPD without single-host parasites.

Figure 7 illustrates the improvement in predictive accuracy between the models with or without  $g$ . Essentially, incorporating uncertainty results in probability estimates for all interactions, undocumented and documented, where the former is penalized proportional to  $g$ . This reduces the overlap in posterior probability densities between interacting and non-interacting pairs, refer to Appendix Figure 12 for the posterior histogram of both categories.



The model with  $g$  outperforms the full model on both AUC and proportion of positive interactions predicted, including and excluding the single-host parasites (Table 2). These results represent the evaluation on the whole dataset, not only the held-out portion as in Section 5.2. The model with  $g$  is able to predict 91.6% of the documented interactions in the 2010 GMPD, approximately 4369 out of 4775 interactions, where the model without  $g$  predicts approximately 250 fewer interactions. By applying the two-sided Wilcoxon signed rank test to differences in AUC, we found the  $p$ -value to be  $< 0.08$  in favour of the model with  $g$  for the GMPD with single-host parasites, and  $< 0.05$  when removing the single-host parasites.

Table 2: Area under the curve and prediction values for the model with(out)  $g$

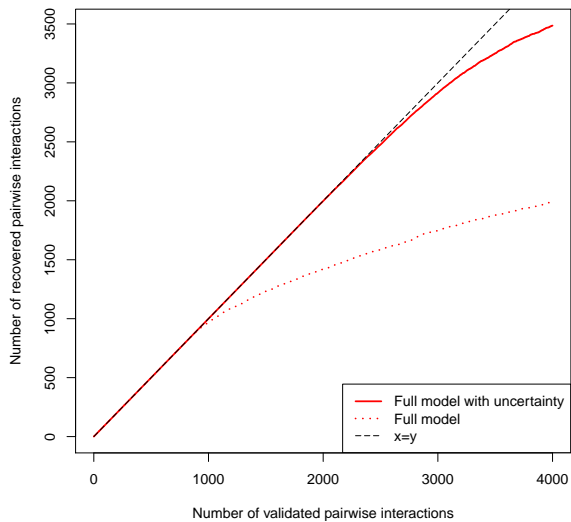
	GMPD			
	no single-host parasites		with single-host parasites	
	AUC	% 1's recovered	AUC	% 1's recovered
with $g$	0.945	86.74	0.955	91.58
without $g$	0.882	81.85	0.937	86.07

Another method of model comparison is through the proportion of recovered interactions from the full data. This can be quantified by sorting all pairwise interactions based on their posterior predictive probabilities, and examining the top  $x$  pairs with the highest predictive probabilities as they represent interactions with highest confidence. By counting the number of true interactions recovered in those  $x$  selected pairs, and by scaling  $x$  from 1 to 3000 we find the model with  $g$  again outperforms the full model by recovering more than double the number of interactions (Figure 8a).

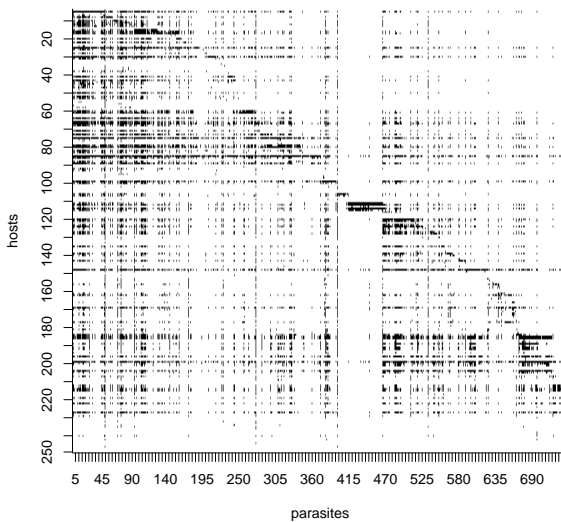
Finally, for comparison with Figure 5, the posterior interaction matrix for the model with  $g$  excluding single-host parasites is shown in Figure 8b. For results with the GMPD including single-host parasites refer to Appendix Figure 13.

## 6 Discussion

We introduced a latent score model for link prediction in ecological networks and illustrate it using a recently published global database of host-parasite interactions. The proposed model is a combination of two separate models, an affinity based exchangeable random networks model overlaid with a Markov network dependence informed by phylogeny (2). The affinity-only model is characterized by independent affinity parameters for each species, while the phylogeny-only model is characterized by a scaled species similarity matrix. Both parts perform reasonably well alone. However, modelling with only the affinity parameters results in a highly dense posterior interaction matrix, in which a slightly elevated affinity parameter results in predicted interactions with all other species. This situation is unlikely from a biological standpoint as species that are known to as-



(a) recovery power



(b) GMPD with  $g$  no single-host parasites

Figure 8: Number of pairwise recovered interactions from the original 2010 GMPD data (left), and the posterior interaction matrix for the 2010 GMPD, excluding single-host parasite, using the model that accounts for uncertainty with  $g$ .

sociate with only particular evolutionary groups will then be predicted to associate with all species. On the other hand, modelling using only with phylogeny allows no independent influence of the number of documented interactions per species. By overlaying the affinity-only model with a phylogeny-only dependence structure, the posterior prediction is significantly improved.

While we incorporated phylogeny as the dependence structure, the model can easily accommodate different similarity matrices or types of dependence in an additive manner. For host-parasite networks, host traits or geographic overlap, or parasite similarity based on phylogeny, taxonomy, or traits may improve prediction (Davies and Pedersen, 2008; Luis et al., 2015; Pedersen et al., 2005). Introducing different similarity measures affects the model characteristics in two ways: it changes the topology of the probability domain, and it increases the number of parameters to estimate due to introduced scaling parameters. The latter is easily integrated since the number of estimated parameters increases by one for each new scaling parameter.

A particular dependence structure that does not require additional data is similarity based on the number of shared interactions, as used in the NN algorithm (Section 5.2). In host-parasite networks, parasite community similarity is often well predicted by evolutionary distance among hosts (Davies and Pedersen, 2008; Gilbert and Webb, 2007). In this case, the NN similarity is likely capturing some of the phylogenetic structure in the network and could be a reasonable approach if a reliable phylogeny is unavailable. However, as phylogeny is estimated independently from the interaction data, it will likely

be more robust to incomplete sampling of the original network than NN type dependence structures.

Many ecological and other real world networks display power-law degree distributions (Albert and Barabasi, 2002). This is also the case with the host-parasite database used in this paper, where both hosts and parasites exhibit power-law degree distributions (Appendix Figure 14). The affinity-only version of the proposed model in (4) has been shown to generate a power-law behaviour when a Generalized Gamma process is used (Brix, 1999; Caron and Fox, 2014; Lijoi et al., 2007). In fact, when  $\gamma_h = \gamma$  for all  $h$ , the affinity-only model behaves much like the Stable Indian Buffet process of Teh and Gorur (2009) that has a power-law behaviour. Nonetheless, we find the full model to show a significant improvement in predictive accuracy over the affinity-only model, though it does not yield a degree distribution with a power-law. However, when accounting for uncertainty in the full model, the posterior predictions we regain a power-law degree distribution for hosts and parasites (Appendix D.5). It would be interesting in future work to explore which other network properties are maintained using this model.

A limitation of observational data is that many networks are based on presence-only data (Morales-Castilla et al., 2015). Thus, the absence of an interaction cannot be taken as evidence that a species pair would not interact given sufficient opportunity. To account for uncertainty in unobserved interactions we extended our full model by estimating the proportion of missing interactions in the observed data. This strengthened the posterior predictive accuracy of the model and proved valuable in reducing the overlap in posterior probability densities for interacting and non-interacting pairs. While the intent of this research is to identify undocumented interactions, this model can also account for uncertainty in observed interactions. In this case, our model may be used to identify weakly supported interactions that are false positives or sampling artifacts in the literature that may benefit from additional investigation. The framework illustrated here is not limited to host-parasite networks, but is well suited to multiple ecological networks such as plant-herbivore, flower-pollinator, or predator-prey interactions. In the case of host-parasite interactions, this approach could form an integral component of proactive surveillance systems for emerging diseases (Farrell et al., 2013).

## 7 Acknowledgements

We like to thank the McGill Statistics-Biology Exchange Group (S-BEX) and organizers Russell Steele, Zofia Taranu, and Amanda Winegardner for fostering an environment that led to this collaboration. We also thank Jonathan Davies and his lab for critical feedback throughout model development and writing, and the Macroecology of Infectious Disease Research Coordination Network (funded by NSF DEB 1316223) for providing early versions of the GMPD. MJF was funded by an NSERC Vanier CGS, and ME by

FQRNT.

## References

- Albert, R. and A. L. Barabasi (2002). Statistical mechanics of complex networks. *Reviews of Modern Physics* 74(1), 47–97.
- Bapst, D. W. (2014). *Modern Phylogenetic Comparative Methods and Their Application in Evolutionary Biology Concepts and Practice*.
- Besag, J. (1974). Spatial interaction and the statistical analysis of lattice systems. *Journal of the Royal Statistical Society. Series B (Methodological)*, 192–236.
- Besag, J. (1986). On the statistical analysis of dirty pictures. *Journal of the Royal Statistical Society. Series B (Methodological)*, 259–302.
- Bickel, P. J. and A. Chen (2009). A nonparametric view of network models and Newman–Girvan and other modularities. *Proceedings of the National Academy of Sciences* 106(50), 21068–21073.
- Brix, A. (1999). Generalized gamma measures and shot-noise Cox processes. *Advances in Applied Probability*, 929–953.
- Caron, F. and E. B. Fox (2014). Sparse graphs using exchangeable random measures. *arXiv preprint arXiv:1401.1137*.
- Chung, F. and L. Lu (2006). Complex graphs and networks, volume 107 of CBMS regional conference series in mathematics. In *Published for the Conference Board of the Mathematical Sciences, Washington, DC*, Volume 144.
- Cleaveland, S., M. K. Laurenson, and L. H. Taylor (2001, jul). Diseases of humans and their domestic mammals: pathogen characteristics, host range and the risk of emergence. *Philosophical transactions of the Royal Society of London. Series B, Biological sciences* 356(1411), 991–999.
- Dallas, T., A. W. Park, and J. M. Drake (2017). Predicting cryptic links in host-parasite networks. *PLOS Computational Biology* 13(5), e1005557.
- Davies, T. J. and A. B. Pedersen (2008). Phylogeny and geography predict pathogen community similarity in wild primates and humans. *Proceedings of the Royal Society - Biological sciences* 275(1643), 1695–701.
- Demšar, J. (2006, December). Statistical comparisons of classifiers over multiple data sets. *Journal of Machine Learning Research* 7, 1–30.

- Farrell, M. J., L. Berrang-Ford, and T. J. Davies (2013, mar). The study of parasite sharing for surveillance of zoonotic diseases. *Environmental Research Letters* 8(1), 015036.
- Farrell, M. J., P. R. Stephens, L. Berrang-Ford, J. L. Gittleman, and T. J. Davies (2015). The path to host extinction can lead to loss of generalist parasites. *Journal of Animal Ecology* 84(4), 978–984.
- Fritz, S. A., O. R. P. Bininda-Emonds, and A. Purvis (2009). Geographical variation in predictors of mammalian extinction risk: big is bad, but only in the tropics. *Ecology letters* 12(6), 538–549.
- Geman, S. and D. Geman (1984). Stochastic relaxation, Gibbs distributions, and the Bayesian restoration of images. *IEEE Transactions on pattern analysis and machine intelligence* (6), 721–741.
- Gilbert, G. S. and C. O. Webb (2007, mar). Phylogenetic signal in plant pathogen-host range. *Proceedings of the National Academy of Sciences of the United States of America* 104(12), 4979–4983.
- Gómez, J. M., M. Verdú, and F. Perfectti (2010, jun). Ecological interactions are evolutionarily conserved across the entire tree of life. *Nature* 465(7300), 918–21.
- Haario, H., E. Saksman, and J. Tamminen (2001). An adaptive Metropolis algorithm. *Bernoulli*, 223–242.
- Harmon, L. J., J. B. Losos, T. Jonathan Davies, R. G. Gillespie, J. L. Gittleman, W. Bryan Jennings, K. H. Kozak, M. A. McPeck, F. Moreno-Roark, T. J. Near, et al. (2010). Early bursts of body size and shape evolution are rare in comparative data. *Evolution* 64(8), 2385–2396.
- Hoff, P. D. (2005). Bilinear mixed-effects models for dyadic data. *Journal of the American Statistical Association* 100(469), 286–295.
- Hoff, P. D., A. E. Raftery, and M. S. Handcock (2002). Latent space approaches to social network analysis. *Journal of the American Statistical Association* 97(460), 1090–1098.
- Jiang, X., D. Gold, and E. D. Kolaczyk (2011). Network-based auto-probit modeling for protein function prediction. *Biometrics* 67(3), 958–966.
- Jordano, P. (2015). Sampling networks of ecological interactions. *bioRxiv*, 025734.
- La Salle, J., K. J. Williams, and C. Moritz (2016). Biodiversity analysis in the digital era. *Philosophical Transactions of the Royal Society B: Biological Sciences* 371(1702), 20150337.

- Lijoi, A., R. H. Mena, and I. Prünster (2007). Controlling the reinforcement in Bayesian non-parametric mixture models. *Journal of the Royal Statistical Society: Series B (Statistical Methodology)* 69(4), 715–740.
- Luis, A. D., T. J. O’Shea, D. T. S. Hayman, J. L. N. Wood, A. A. Cunningham, A. T. Gilbert, J. N. Mills, and C. T. Webb (2015, aug). Network analysis of host-virus communities in bats and rodents reveals determinants of cross-species transmission. *Ecology Letters* 18(11), 1153–1162.
- Morales-Castilla, I., M. G. Matias, D. Gravel, and M. B. Araújo (2015). Inferring biotic interactions from proxies. *Trends in ecology & evolution* 30(6), 347–356.
- Olival, K. J., P. R. Hosseini, C. Zambrana-Torrel, N. Ross, T. L. Bogich, and P. Daszak (2017). Host and viral traits predict zoonotic spillover from mammals. *Nature* 546(7660), 646–650.
- Pagel, M. (1999). Inferring the historical patterns of biological evolution. *Nature* 401(6756), 877–884.
- Parrish, C. R., E. C. Holmes, D. M. Morens, E.-C. Park, D. S. Burke, C. H. Calisher, C. a. Laughlin, L. J. Saif, and P. Daszak (2008, sep). Cross-species virus transmission and the emergence of new epidemic diseases. *Microbiology and molecular biology reviews : MMBR* 72(3), 457–70.
- Pedersen, A. B., S. Altizer, M. Poss, A. A. Cunningham, and C. L. Nunn (2005). Patterns of host specificity and transmission among parasites of wild primates. *International journal for parasitology* 35(6), 647–57.
- Pedersen, A. B., K. E. Jones, C. L. Nunn, and S. Altizer (2007, oct). Infectious diseases and extinction risk in wild mammals. *Conservation Biology* 21(5), 1269–79.
- Poelen, J. H., J. D. Simons, and C. J. Mungall (2014). Global biotic interactions: An open infrastructure to share and analyze species-interaction datasets. *Ecological Informatics* 24, 148 – 159.
- Ricci, F., L. Rokach, and B. Shapira (2011). *Introduction to recommender systems handbook*. Springer.
- Robert, C. and G. Casella (2013). *Monte Carlo statistical methods*. Springer Science & Business Media.
- Stephens, P. R., P. Pappalardo, S. Huang, J. E. Byers, M. J. Farrell, A. Gehman, R. R. Ghai, S. E. Haas, B. Han, A. W. Park, J. P. Schmidt, S. Altizer, V. O. Ezenwa, and C. L. Nunn (2017). Global Mammal Parasite Database version 2.0. *Ecology* 98(February), 2017.

- Swendsen, R. H. and J.-S. Wang (1987). Nonuniversal critical dynamics in Monte Carlo simulations. *Phys. Rev. Lett.* *58*, 86–88.
- Teh, Y. W. and D. Gorur (2009). Indian buffet processes with power-law behavior. In *Advances in neural information processing systems*, pp. 1838–1846.
- Wardeh, M., C. Risley, M. K. McIntyre, C. Setzkorn, and M. Baylis (2015). Database of host-pathogen and related species interactions, and their global distribution. *Scientific data* *2*.
- Weir, I. S. and A. N. Pettitt (2000). Binary probability maps using a hidden conditional autoregressive Gaussian process with an application to Finnish common toad data. *Journal of the Royal Statistical Society: Series C (Applied Statistics)* *49*(4), 473–484.
- Wiens, J. J., D. D. Ackerly, A. P. Allen, B. L. Anacker, L. B. Buckley, H. V. Cornell, E. I. Damschen, T. Jonathan Davies, J.-A. Grytnes, S. P. Harrison, B. a. Hawkins, R. D. Holt, C. M. McCain, and P. R. Stephens (2010). Niche conservatism as an emerging principle in ecology and conservation biology. *Ecology letters* *13*(10), 1310–24.

## Appendix A Model general settings

Let  $\mathbf{Z}$  be an  $H \times J$  host-parasite interaction matrix, where the binary variable  $z_{hj}$  denotes whether an interaction between host  $h$  and parasite  $j$  has been observed. Let  $\phi(T_{hi}, \eta)$  be a transformation of the evolutionary distance  $T_{hi}$ , between hosts  $h$  and  $i$ , tuned by the parameter  $\eta$ . Moreover, let  $\gamma_h > 0$  be the affinity parameter of host  $h$  and  $\rho_j > 0$  be the affinity parameter of parasite  $j$ . Following the conditional full model of (4) as

$$\mathbf{P}(z_{hj} = 1 \mid \mathbf{Z}_{-(hj)}) = 1 - \exp(-\tau_{hj}) \quad (16)$$

where  $\tau_{hj} = \gamma_h \rho_j \delta_{hj}(\eta)$ , and  $\delta_{hj}(\eta)$  as in (2). Define a latent score  $s_{hj}$  as in (5). Such a characterization prompts a conditional joint distribution of the form

$$\begin{aligned} \mathbf{P}(z_{hj} = 1, s_{hj} \mid \mathbf{Z}_{-(hj)}) &= \mathbf{P}(z_{hj} = 1 \mid s_{hj})\mathbf{p}(s_{hj} \mid \mathbf{S}_{-(hj)}) = \mathbf{p}(s_{hj} \mid \mathbf{S}_{-(hj)})\mathbb{I}_{\{s_{hj} > 0\}} \\ \mathbf{P}(z_{hj} = 0, s_{hj} \mid \mathbf{Z}_{-(hj)}) &= \mathbf{P}(z_{hj} = 0 \mid s_{hj})\mathbf{p}(s_{hj} \mid \mathbf{S}_{-(hj)}) = \mathbf{p}(s_{hj} \mid \mathbf{S}_{-(hj)})\mathbb{I}_{\{s_{hj} = 0\}} \end{aligned} \quad (17)$$

Moreover, it can be verified that

$$\mathbf{p}(s_{hj} \mid z_{hj}, \mathbf{Z}_{-(hj)}) = \begin{cases} \frac{1}{1 - \exp(-\tau_{hj})} \mathbf{p}(s_{hj} \mid \mathbf{S}_{-(hj)})\mathbb{I}_{\{s_{hj} > 0\}} & z_{hj} = 1 \\ \frac{1}{\exp(-\tau_{hj})} \mathbf{p}(s_{hj} \mid \mathbf{S}_{-(hj)})\mathbb{I}_{\{s_{hj} = 0\}} & z_{hj} = 0 \end{cases}$$

It remains to define the distribution of  $s_{hj} \mid \mathbf{Z}_{-(hj)}$  to satisfy the property that

$$\mathbf{P}(z_{hj} = 1 \mid \mathbf{Z}_{-(hj)}) = 1 - \exp(-\tau_{hj}) = \int_{\mathbb{R}} \mathbf{p}(s \mid \mathbf{S}_{-(hj)}) \mathbb{I}_{\{s>0\}} \mathbf{d}s$$

One possible choice is the zero-inflated Gumbel density as

$$\mathbf{p}(s_{hj} \mid \mathbf{S}_{-(hj)}) = \tau_{hj} \exp(-s_{hj} - \tau_{hj} e^{-s_{hj}}) \mathbb{I}_{\{s_{hj}>0\}} + \exp(-\tau_{hj}) \mathbb{I}_{\{s_{hj}=0\}}$$

The latent score is used only as a modelling tool to make the joint distribution more tractable, as

$$\begin{aligned} \mathbf{p}(z_{hj}, s_{hj} \mid \mathbf{Z}_{-(hj)}) &= \left[ \tau_{hj} \exp\left(-s_{hj} - \tau_{hj} e^{-s_{hj}}\right) \mathbb{I}_{\{s_{hj}>0\}} \right]^{z_{hj}} \left[ \exp(-\tau_{hj}) \mathbb{I}_{\{s_{hj}=0\}} \right]^{1-z_{hj}} \\ &= \tau_{hj}^{z_{hj}} \exp\left(-s_{hj} - \tau_{hj} e^{-s_{hj}}\right) \end{aligned} \tag{18}$$

## Appendix B Existence of the joint distribution

**Theorem 1.** *Hammersley-Clifford, (Robert and Casella, 2013).*

*Under marginal positively conditions, the joint distribution of random variables  $X = (x_1, x_2, \dots, x_n)$  is proportional to*

$$\frac{\mathbf{P}(X)}{\mathbf{P}(X^*)} = \prod_{i=1}^n \frac{\mathbf{P}(x_i \mid x_1, \dots, x_{i-1}, x_{i+1}^*, \dots, x_n^*)}{\mathbf{P}(x_i^* \mid x_1, \dots, x_{i-1}, x_{i+1}^*, \dots, x_n^*)} \tag{19}$$

where  $x_i^*$  are fixed observations, for example  $x_i^* = 1$ .

In regards to conditional probability in (16), assume the phylogeny-only model where  $\tau_{hj} = \delta_{hj}(\eta)$ , and  $\delta_{hj}(\eta)$  as in (2). Since each column of  $\mathbf{Z}$  is independent, it suffices to show that the joint distribution exists for each column. Applying the Hammersley-Clifford theorem, we have

$$\frac{\mathbf{P}(z_{hj} \mid z_{1j}, \dots, z_{(h-1)j}, z_{(h+1)j}^*, z_{Hj}^*)}{\mathbf{P}(z_{hj}^* \mid z_{1j}, \dots, z_{(h-1)j}, z_{(h+1)j}^*, z_{Hj}^*)} = \left[ \frac{\exp(-\bar{\tau}_{hj})}{1 - \exp(-\bar{\tau}_{hj})} \right]^{1-z_{hj}},$$

where  $z_{hj}^* = 1$  and

$$\bar{\tau}_{hj} = \sum_{i=1}^{h-1} \frac{z_{ij}}{\phi(T_{hi}, \eta)} + \sum_{i=h+1}^H \frac{1}{\phi(T_{hi}, \eta)}, \quad \bar{\tau}_{1j} = \sum_{i=2}^H \frac{1}{\phi(T_{1i}, \eta)}, \quad \bar{\tau}_{Hj} = \sum_{i=1}^{H-1} \frac{z_{ij}}{\phi(T_{Hi}, \eta)}.$$

Essentially, by removing the event of no interactions, as  $\mathbf{z}_h = (0, 0, \dots, 0)$ , and setting  $\bar{\tau}_{hj} = 1$  whenever it is 0, the joint distribution exists.



## B.1 Conditional joint distribution and ICM

The Iterated Conditional Modes (ICM) of [Besag \(1986\)](#) algorithm is used to update the parameters of conditionally independent parts of the joint distribution. The neighbourhood dependence represented by host-phylogeny is column specific, thus the conditional modes could be the rows of  $\mathbf{Z}$ .

Elements of every row in an  $H \times J$  matrix  $\mathbf{Z}$  are independently distributed, having the joint conditional density for the  $h$ -th row as

$$\mathbf{p}_h(\mathbf{z}_h, \mathbf{s}_h \mid \mathbf{Z}_{-(h.)}) = \prod_{j=1}^J \mathbf{p}(z_{hj}, s_{hj} \mid \mathbf{Z}_{-(h.)}), \quad (20)$$

where  $\mathbf{z}_h = (z_{h,1}, \dots, z_{h,J})$ ,  $\mathbf{s}_h = (s_{h1}, \dots, s_{hJ})$  and  $\mathbf{Z}_{-(h.)}$  is the interaction matrix  $\mathbf{Z}$  excluding the  $h$ -th row. Only the column parameters ( $\rho_j$ ) are affected by partitioning the row modes of  $\mathbf{Z}$ . A complete cycle over the rows of  $\mathbf{Z}$  results in a sample for each row parameter ( $\gamma_h$ ),  $H$  samples for each column parameter ( $\rho_j$ ) and the tree scaling parameter ( $\eta$ ). A pointwise posterior estimate for each parameter is obtained by averaging over the sample set.

## B.2 Parametrization using an exponential distribution

Rather than using a Gumbel distribution, one can achieve an equivalent parametrization using the exponential distribution. Suppose that  $z_{hj}$  is completely determined by a latent variable  $u_{hj}$ , such that

$$z_{hj} = \begin{cases} 1 & u_{hj} < 1 \\ 0 & u_{hj} = 1. \end{cases}$$

A possible choice for the distribution of  $u_{hj} \mid \mathbf{Z}_{-(hj)}$  is the density of an inflated exponential distribution at 1, as

$$\mathbf{p}(u_{hj} \mid \mathbf{Z}_{-(hj)}) = \tau_{hj} \exp\left(-\tau_{hj} u_{hj}\right) \mathbb{I}_{\{u_{hj} < 1\}} + \exp\left(-\tau_{hj}\right) \mathbb{I}_{\{u_{hj} = 1\}}.$$

The joint distribution becomes

$$\begin{aligned} \mathbf{p}(z_{hj}, u_{hj} \mid \mathbf{Z}_{-(hj)}) &= \left[ \tau_{hj} \exp\left(-\tau_{hj} u_{hj}\right) \mathbb{I}_{\{u_{hj} < 1\}} \right]^{z_{hj}} \left[ \exp\left(-\tau_{hj}\right) \mathbb{I}_{\{u_{hj} = 1\}} \right]^{1-z_{hj}} \\ &= \tau_{hj}^{z_{hj}} \exp\left(-\tau_{hj} u_{hj}\right). \end{aligned}$$

## Appendix C Latent score sampling with uncertainty

By modelling the uncertainty parameter  $g$  as

$$\mathbf{p}(z_{hj} = 0 \mid s_{hj}, g) = \begin{cases} 1, & \text{if } s_{hj} = 0 \\ g, & \text{if } s_{hj} > 0. \end{cases}$$

One arrives at the conditional joint distributions

$$\begin{aligned} \mathbf{P}(z_{hj} = 1, s_{hj} \mid g, \mathbf{Z}_{-(hj)}) &= \mathbf{P}(z_{hj} = 1 \mid g, s_{hj})\mathbf{p}(s_{hj} \mid \mathbf{Z}_{-(hj)}) \\ &= \mathbf{p}(s_{hj} \mid \mathbf{Z}_{-(hj)})\mathbb{I}_{\{s_{hj}>0\}} \\ \mathbf{P}(z_{hj} = 0, s_{hj} \mid g, \mathbf{Z}_{-(hj)}) &= \mathbf{P}(z_{hj} = 0 \mid g, s_{hj})\mathbf{p}(s_{hj} \mid \mathbf{Z}_{-(hj)}) \\ &= \mathbf{p}(s_{hj} \mid \mathbf{Z}_{-(hj)}) \left[ g\mathbb{I}_{\{s_{hj}>0\}} + \mathbb{I}_{\{s_{hj}=0\}} \right]. \end{aligned} \tag{21}$$

The conditional sampling of the latent truncated score variable  $s_{hj}$  becomes

$$\begin{aligned} \mathbf{p}(s_{hj} \mid z_{hj}, \mathbf{Z}_{-(hj)}, g) &= \frac{\mathbf{P}(z_{hj} \mid s_{hj}, g) \cdot \mathbf{p}(s_{hj} \mid \mathbf{Z}_{-(hj)})}{\int \mathbf{P}(z_{hj} \mid s, g) \cdot \mathbf{p}(s \mid \mathbf{Z}_{-(hj)}) \mathbf{d}s} \\ &= C \cdot \mathbf{p}(s_{hj} \mid \mathbf{Z}_{-(hj)}), \end{aligned}$$

Such that

$$\begin{aligned} C &= \frac{\mathbf{P}(z_{hj} \mid s_{hj}, g)}{\int \mathbf{P}(z_{hj} \mid s, g) \cdot \mathbf{p}(s \mid \mathbf{Z}_{-(hj)}) \mathbf{d}s} \\ &= \frac{\mathbf{P}(z_{hj} \mid s_{hj}, g)}{\int_{s>0} \mathbf{P}(z_{hj} \mid s, g) \cdot \mathbf{p}(s \mid \mathbf{Z}_{-(hj)}) \mathbf{d}s + \int_{s\leq 0} \mathbf{P}(z_{hj} \mid s, g) \cdot \mathbf{p}(s \mid \mathbf{Z}_{-(hj)}) \mathbf{d}s} \\ &= \begin{cases} \frac{\mathbf{P}(z_{hj} \mid s_{hj}, g)}{\int_{s>0} 1 \cdot \mathbf{p}(s \mid \mathbf{Z}_{-(hj)}) \mathbf{d}s + \int_{s\leq 0} 0 \cdot \mathbf{p}(s \mid \mathbf{Z}_{-(hj)}) \mathbf{d}s}, & \text{when } z_{hj} = 1, \\ \frac{\mathbf{P}(z_{hj} \mid s_{hj}, g)}{\int_{s>0} g \cdot \mathbf{p}(s \mid \mathbf{Z}_{-(hj)}) \mathbf{d}s + \int_{s\leq 0} 1 \cdot \mathbf{p}(s \mid \mathbf{Z}_{-(hj)}) \mathbf{d}s}, & \text{when } z_{hj} = 0, \end{cases} \\ &= \begin{cases} \frac{1}{\psi(\bar{s}_{hj})}, & s_{hj} > 0, \quad z_{hj} = 1, \\ 0, & s_{hj} = 0, \quad z_{hj} = 1, \\ \frac{g}{g\psi(\bar{s}_{hj}) + 1 - \psi(\bar{s}_{hj})}, & s_{hj} > 0, \quad z_{hj} = 0, \\ \frac{1}{g\psi(\bar{s}_{hj}) + 1 - \psi(\bar{s}_{hj})}, & s_{hj} = 0, \quad z_{hj} = 0, \end{cases} \end{aligned}$$

## Appendix D Additional results for GMPD

### D.1 Basic predictive accuracy under alternative phylogeny transformational models

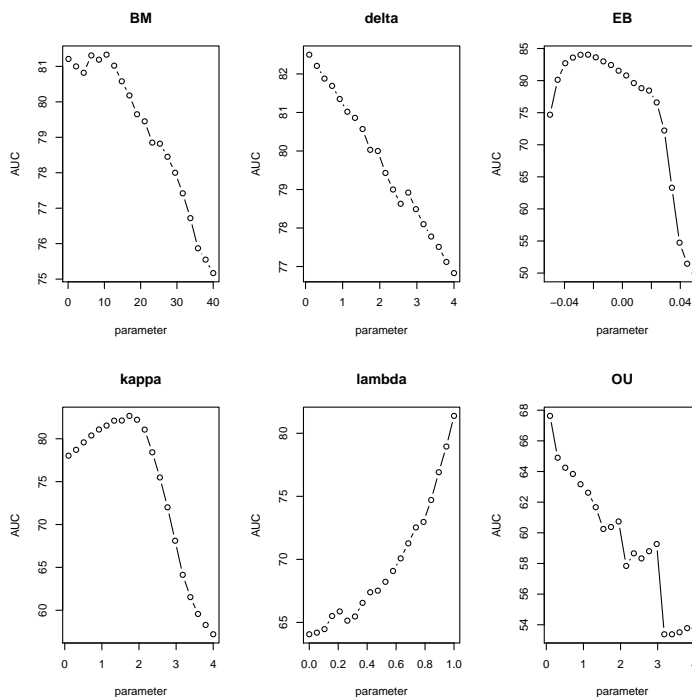


Figure 9: Grid search over the tree transformation parameter for basic AUC results under the phylogeny-only model (paper Eq. (2)) with GMPD for different phylogeny transformational models: Brownian motion (BM), delta, early-bust (EB), kappa, lambda, and the Ornstein-Uhlenbeck (OU) models.

## D.2 Posteriors and trace plots

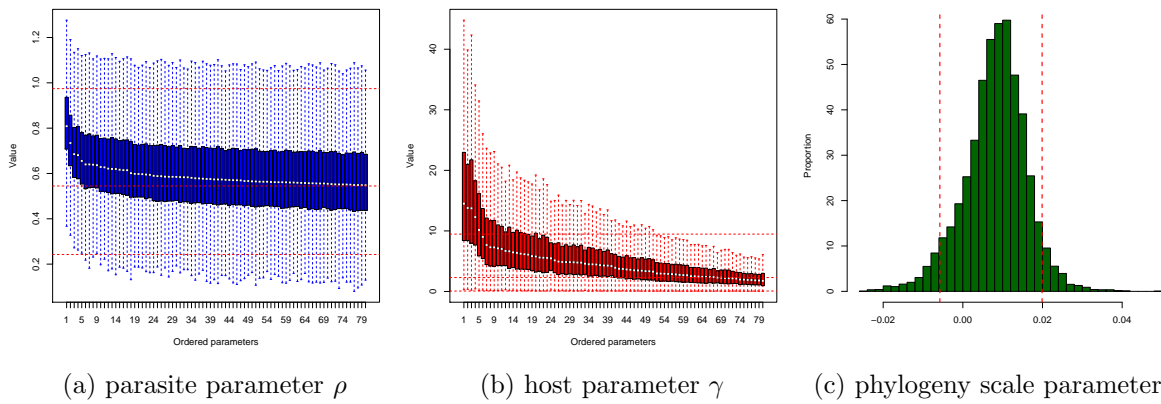


Figure 10: Boxplots of posterior estimates for the host and parasite parameters with the 80 highest medians, and the posterior distribution of the EB model parameter, dashed lines are the mean posterior and 95% credible intervals.

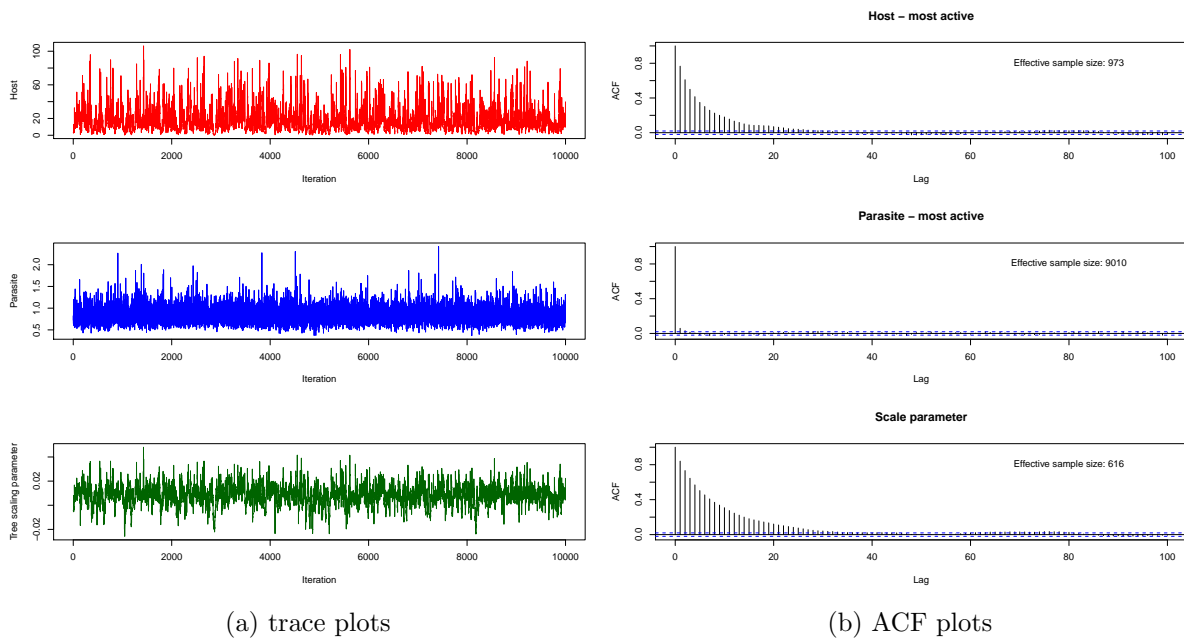


Figure 11: Trace plots (left panel), auto-correlation plots and effective sample sizes (right panel): host (top) and parasite (middle) of highest median posterior, and phylogeny EB model parameter (bottom).

### D.3 Uncertainty - histograms

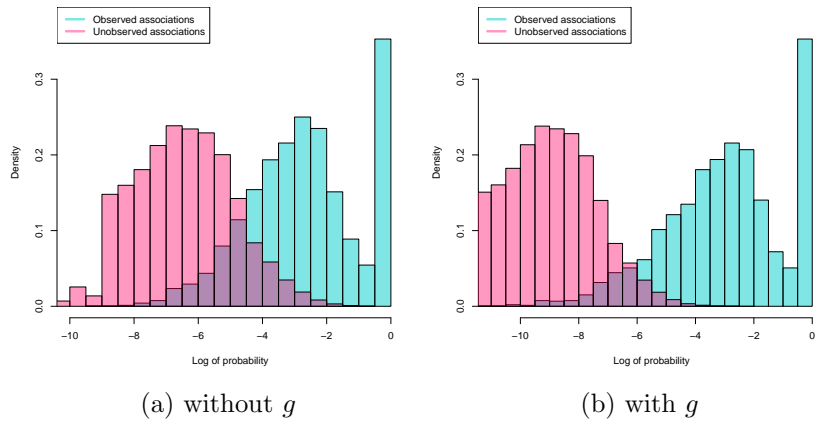


Figure 12: Comparison in posterior log-probability between observed and unobserved interactions, for the model without  $g$  (left) and with  $g$  (right), for GMPD with single-host parasites.

### D.4 ROC with and without $g$

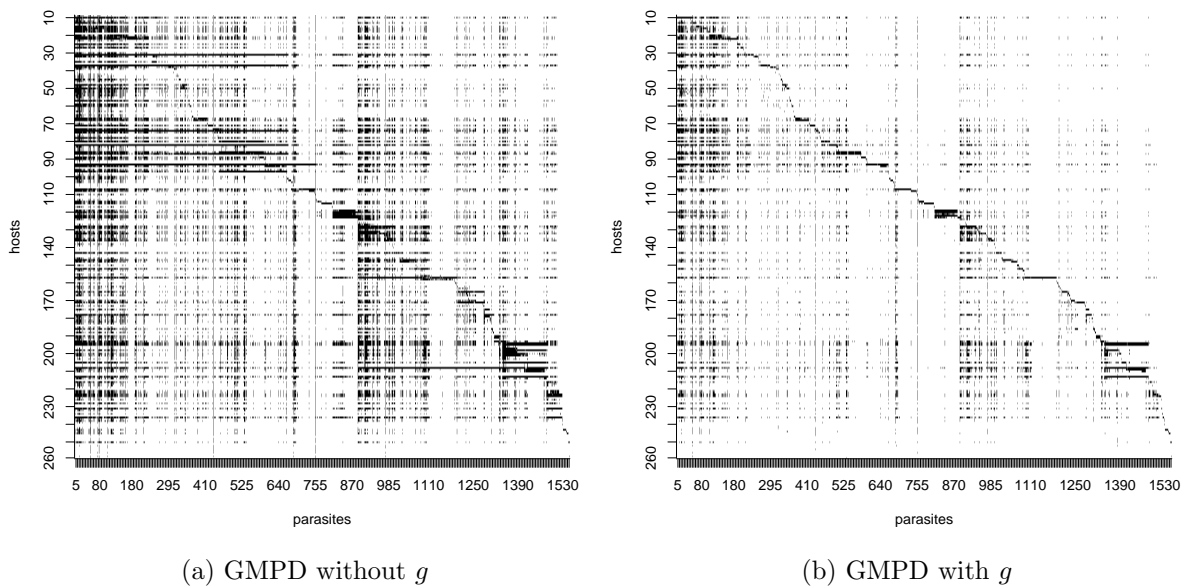
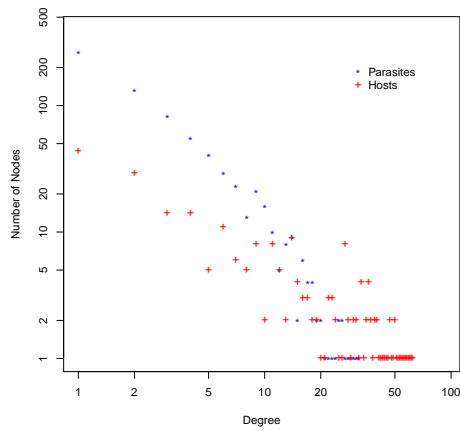


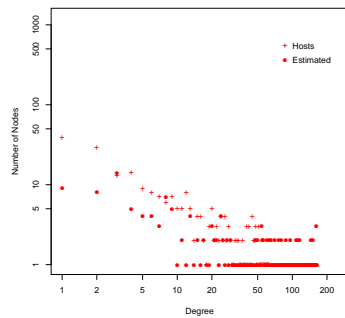
Figure 13: Posterior association matrices for the 2010 GMPD with single-host parasites.

## D.5 Posterior degree distribution

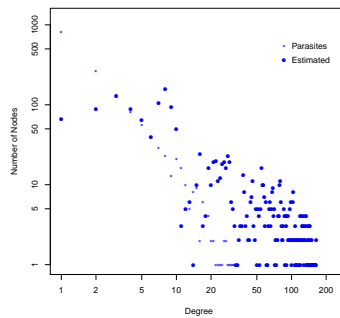


(a) GMPD

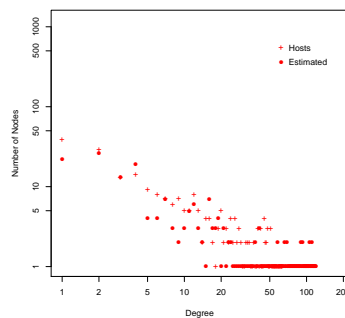
Figure 14: Degree distribution of hosts (red crosses) and parasites (blue stars) on log-scale, for the GMPD.



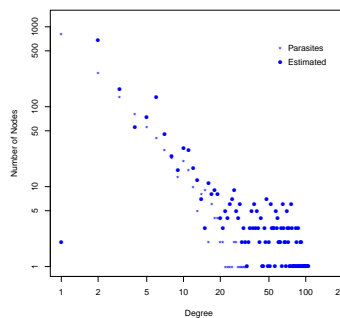
(a) Hosts - full model



(b) Parasites - full model



(c) Hosts - full model with  $g$



(d) Parasites - full model with  $g$

Figure 15: Comparison of degree distribution on log-scale, for the full model (without accounting for uncertainty) and the model with  $g$ , 2010 GMPD with single-host parasites.